PROCEEDINGS OF SPIE

SPIEDigitalLibrary.org/conference-proceedings-of-spie

Modeling and realization of photonic structures for silicon-based tandem solar cells

Höhn, Oliver, Hauser, Hubert, Tucher, Nico, Müller, Ralph, Bläsi, Benedikt

Oliver Höhn, Hubert Hauser, Nico Tucher, Ralph Müller, Benedikt Bläsi, "Modeling and realization of photonic structures for silicon-based tandem solar cells," Proc. SPIE 11275, Physics, Simulation, and Photonic Engineering of Photovoltaic Devices IX, 1127502 (3 March 2020); doi: 10.1117/12.2551034

SPIE.

Event: SPIE OPTO, 2020, San Francisco, California, United States

Modeling and Realization of Photonic Structures for Silicon Based Tandem Solar Cells

Oliver Höhn*[a], Hubert Hauser[a], Nico Tucher[a], Ralph Müller[a], Benedikt Bläsi[a]
[a]Fraunhofer Institute for Solar Energy Systems ISE; Heidenhofstr. 2, 79110 Freiburg, Germany

ABSTRACT

Different photonic light trapping structures realized by a combination of interference- and nanoimprint-lithography as well as based on self-organization processes are presented. Their potential as rear side light trapping structures for silicon based tandem solar cells is evaluated based on the comparison of EQE measurements and optical modeling. The photonic structure used in the current world record III-V silicon tandem solar cell is a metallic crossed grating with 1µm period. This structure is shown in detail and acts as benchmark for the comparison of the concepts. Finally, the requirements for a successful implementation of photonic structures in highest efficiency solar cells are shown.

Keywords: Light Trapping, Nanoimprint lithography, OPTOS, Self-organisation, silicon-based tandem solar cells, photonic contacts.

1. INTRODUCTION

Silicon based tandem solar cells are one path towards next generation photovoltaics. To tap the full potential of these devices, photon management in the silicon bottom solar cell is crucial especially for the weakly absorbed photons close to the silicon band gap. One concept for photon management is to implement a photonic structure at the rear side that at the same time acts as the contact. Such a structure is called "photonic contact" in the following.
We could confirm the advantage of such a photonic contact by raising the efficiency of a triple junction III/V silicon tandem solar cell by $1.8\%_{absolute}$ to 34.1[1, 2]. The crossed grating with a period of 1 µm used for the record devices and also in this work was realized by a combination of laser interference lithography as mastering technique [3], Roller-Nanoimprint Lithography (NIL) [4, 5] with subsequent residual layer etching and silver evaporation to establish a photonic rear side contact [2].
The grating period of 1 µm has been found as optimum for diffractive light trapping in silicon solar cells in several works [6–8].
Apart from this, quasi-periodic structures can cause a ring like scattering profile [9, 10] and in principle can lead to similar light trapping properties. One possible process for the realization of disordered structures with tunable size and pitch distributions is based on the phase separation of two immiscible polymers in a solution [11, 12]. Such structures showing a tailored disorder were already applied to thin film solar cells [13]. In the following two different approaches for photonic contacts are shown:

(1) The diffractive grating used in the current record devices [2] and
(2) a newly developed self-organized photonic contact [14] with a pseudo period[1] of approximately 1 µm based on the phase separation of polystyrene (PS) and poly(methyl methacrylate) (PMMA).

The processing routes are described, EQE measurements are shown and finally the potential current gain for silicon bottom solar cells with more industrially relevant thicknesses in the range of 150-180 µm is estimated with the help of OPTOS [8] simulations that were calibrated with the experimental results.

In order to achieve highest efficiencies with the help of light trapping structures, it is not sufficient to just increase the generated current density as compared to a planar device. Additionally, the voltage and the fill factor must not be affected negatively, or at least a decrease in voltage or fill factor has to be overcompensated by the increased current density of the device [15]. This is a general rule that always has to be considered, when implementing light trapping structures into highly efficient devices.

[1] defined as the predominant feature size deduced from the auto correlation function of AFM images of the structure

Physics, Simulation, and Photonic Engineering of Photovoltaic Devices IX, edited by Alexandre Freundlich, Masakazu Sugiyama, Stéphane Collin, Proc. of SPIE Vol. 11275, 1127502 · © 2020 SPIE
CCC code: 0277-786X/20/$21 · doi: 10.1117/12.2551034

2. PROCESSING ROUTE

The 280µm thick silicon bottom solar cell used as test structure has planar tunnel oxide passivated contact layers on both sides (TOPCon [16]). Using a both side planar device principally allows for the highest voltage, however light trapping concepts other than the commonly used wet-chemically etched random pyramids are required in this case.

While usually on top of these bottom cells the top cell is attached with wafer bonding [2] or direct growth [17], this is not done for testing different rear side structures experimentally. In the case of strongly absorbing III-V top solar cells, it is in very good approximation sufficient to test the structures only for the silicon bottom solar cell and only account for a current gain in the part of the silicon EQE at energies below the band gap of the top solar cells, as light trapping at the rear side only affects the silicon solar cell. This is especially true, if the transmission through the top cell as well as the antireflective properties are very good. This is the case for the above mentioned records cells, where the top solar cells are attached with direct wafer bonding [2].

The processing routes for the NIL-based photonic contact and the self-organized photonic contact differ in process steps as well as complexity. The NIL-route is more elaborate, but a well-defined periodic structure can be realized. The self-organization route is extremely easy, but there are limitations to the structure, especially perfectly periodic structures cannot be realized.

2.1 Imprint based photonic contact

Before imprinting a sample, a PDMS stamp has to be fabricated. This is done by replicating a master structure originated by laser interference lithography [3, 18, 19]. After photoresist coating of the sample (in our case the rear side of the silicon bottom cell) the imprint is done with a Roller-NIL tool developed at Fraunhofer ISE [4] using the PDMS stamp including a thermally assisted UV curing of the SU8-2002 photoresist [5]. Afterwards the remaining residual photoresist layer is etched and the sample is metallized. This etching is necessary to allow for an ohmic contact to the silicon bottom solar cell. A sketch of the process can be found in Figure 1. More details about the process and process parameters can be found in the work of Cariou et al. [2] and Hauser et al. [14].

Note that only the steps after the stamp fabrication have to be repeated for each sample – after the highly complex master fabrication a large quantity of PDMS stamps can be replicated and each stamp can be used for a large number of imprints.

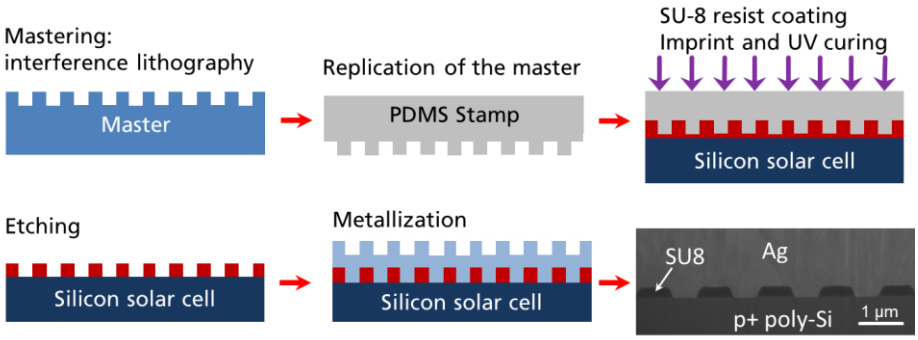

Figure 1 Sketch of the process flow for realizing a NIL-based photonic contact

2.2 Self-organized photonic contact

The processing route for the self-assembled diffuser is much simpler:

The sample – in our case the rear side of the silicon bottom solar cell – is coated with a mixture of PMMA with a molar weight of 15 kg/mol and PS with a molar weight of 35 kg/mol in a mixing ration of 1/1 dissolved in methyl-ethyl-ketone (MEK) with a polymer content of 2 wt.% in the solution. Afterwards one of the two polymers can be removed selectively. For the investigated samples PMMA was solved in acetic acid, resulting in a PS structure which then was metalized with silver. A sketch of the processing route is shown in Figure 2, a SEM image of the resulting structure before metallization is shown in Figure 3. A more detailed description of the process can be found [14].

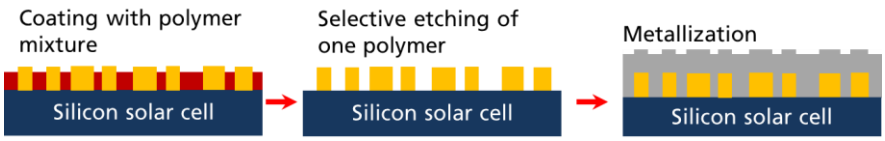

Figure 2 Sketch of the process flow for realizing a self-organized photonic contact

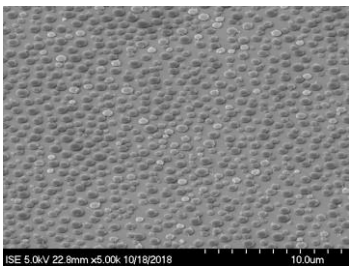

Figure 3 SEM image of a self-assembled polymer structure before metallization

So, compared to the NIL approach, no mastering, no stamp fabrication, and – more important – no NIL-step is needed. In terms of repetitive steps one step can be saved. Additionally, instead of the residual layer etching in the NIL process a selective etching step is performed, which is due to the selectivity of the etching solution a much simpler process step.

2.3 Realized cell structures

In Figure 4 sketches of the realized cell structures are shown. Both concepts were realized on TOPCon silicon solar cells, however the front side contacting differs a bit, which also is the reason for the difference in the EQE level and the different IV measurement methods. While for the self-assembled rear side a very coarse silver grid at the front side was realized using a shadow mask for the Ag evaporation, for the structures with the rear side grating a photolithographic grid was applied on an ITO layer to act as transparent conductive oxide for improved lateral conductivity.

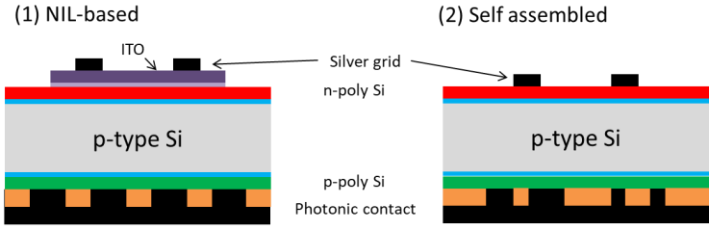

Figure 4 Sketch of the realized test structures for the NIL-based and the self-assembled photonic contact

The direct silver metallization is much simpler, but does not allow for light IV measurements but only for Suns-Voc measurements, which is a well-established measurement method for the characterization of solar cells especially regarding the open circuit voltage [20, 21]. The metallization with an additional ITO allows for all measurements, but is far more complex and more sensitive to process variations and other sources of error.

3. MODELING METHOD

For modeling the solar cells with the self-assembled photonic contact, the OPTOS [8, 22] formalism was used. The rear side was described using a simple Phong-scatter model as presented in [23]. Parasitic losses at the structured metal are deduced from the planar case. As this is just an empiric scattering model and no description of the structure, the error is quite large. Thus the scattering angle ($\gamma_{scatter}$ relative to $\theta_{out} = \theta_{in}$ that describes the decay of the scattered intensity to 1/e as compared to the intensity at the angle $\theta_{out} = \theta_{in}$) was varied and the best fitting curve was used for subsequent modeling. The scattering behavior of the Phong-scatterer can be described by:

$$f_{R,Phong} = \cos^{W}\left(\theta_{out} - \theta_{in}\right), \tag{1}$$

while the scattering angle is defined as

$$\gamma_{scatter} = \arccos\left[\left(\frac{1}{e}\right)^{1/W}\right]. \tag{2}$$

A depiction of the scattering distribution and the scattering angle can be found in Figure 5.

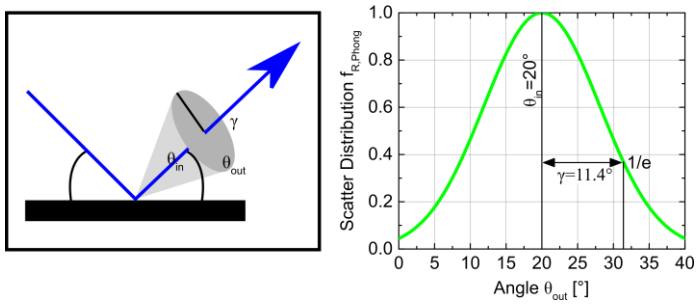

Figure 5 Depiction of the scatter distribution $f_{R,Phong}$ and the scatter angle $\gamma_{scatter}$. For an angle on incidence of 20° and a scatter angle of 11.4° [23].

4. RESULTS

After the realization of the rear side structures on both-side planar silicon solar cells, EQE measurements were performed. From the EQE measurements the current gain caused by the gratings can be extracted, when comparing to reference cells with a planar rear silver mirror. As mentioned above, just achieving a current gain is not enough. At the same time also fill factor (FF) and open circuit voltage (V_{oc}) should not be deteriorated. Thus Suns-Voc measurements for the cells with self-organized photonic contact were performed and light IV measurements were done for the cells with the NIL-based photonic contact. V_{oc} and FF were compared to the corresponding references.
Afterwards the EQE of the self-organized structure was compared to the absorptance simulated with the OPTOS model described in section 3.

4.1 EQE, Voc and FF measurements at single junction devices

In Figure 6 the EQE measurement results are shown for both structures. For the NIL-based photonic contact, different metals and etching methods (wet-chemical piranha etching and oxygen plasma etching) were tested [14]. For the self-organized sample only silver was evaluated as rear side metallization. The different maximal height of the EQEs in the two cases solely is caused by the different front side as mentioned above.

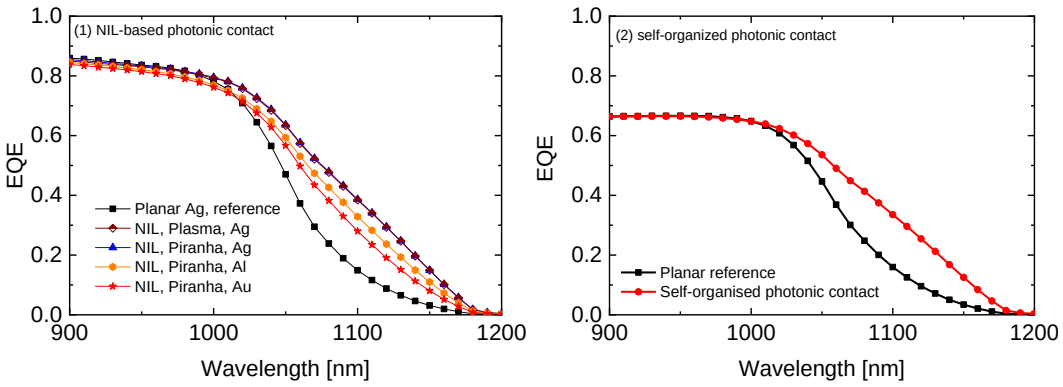

Figure 6 EQE measurements of the test structures with the (1) NIL-based photonic contact with different metals and (2) the self-organized photonic contact with silver metallization

It was found for the NIL-based photonic contact that silver as metal leads to the highest improvement in current. A current gain of 1.1 mA/cm² was measured for the silver, which is in excellent agreement to the current gain that also was

measured in the device mentioned in [2], where the same structure was implemented into a 3-jucntion solar cell. This again confirms that testing structures on single junction silicon solar cells with comparable cell architectures is valid. The current gain of the self-organized photonic contact was measured to be 0.6 mA/cm². When correcting for the imperfect front side reflectance, this leads to a potential current gain of 1.1 mA/cm². Thus it can be concluded that with the much simpler processing route of the self-organized diffuser the same current gains can be achieved as with the currently best implemented NIL-based photonic contact. Note that there might be other complex photonic structures that allow for even higher current gains, but these were until now not successfully implemented into a highly efficient solar cell without deteriorating either FF or V_{oc}.

All cell results can be found in Table 1. From there it can be seen that the FF as well as the voltage were not harmed after implementing the photonic rear side contact using one of the two methods. The lower FF for the cells with NIL-based photonic contact and their reference are caused by a dark emitter, as the cells were not separated well due to some processing issues in this more complex structure. Still one can see that the FF is maintained after processing, when comparing the cells to the corresponding reference. This again is in good agreement with the results in the work of Cariou et al.[2], where the high FF was maintained after implementing the diffractive rear side photonic contact into a III-V silicon tandem solar cell.

Table 1 Measurement results of the different cells. The current gains are taken from integrated EQEs weighted with the AM1.5g spectrum. No deterioration of V_{oc} or FF can be found within the measurement error for the different photonic contacts. In the case of the SunsVoc results the FF and V_{oc} are pseudo values.

	Voc [mV]	FF [-]	Current gain [mA/cm²]
NIL-based: Light IV measurements			
Ref	713	0.74	
Piranha etch + Ag	711	0.73	1.1
Plasma etch + Ag	704	0.70	1.1
Piranha etch + Al	711	0.73	0.7
Piranha etch + Au	710	0.74	0.5
Self-organized : SunsVoc results			
Ref	672	0.81	-
Self-organized	673	0.82	0.6

From these results it can be concluded that all requirements for the successful implementation of a photonic light management structure into a highly efficient device were achieved: The current could be increased, while at the same time neither FF nor V_{oc} are deteriorated.

4.2 Comparison to modeling

In Figure 7 the measured EQE is compared to absorptance modelling using the OPTOS formalism. One can see that the reference device with a planar silver mirror can be described with high accuracy. The device with the self-organized photonic contact can be modelled well, when assuming a Phong-scatterer at the rear side. The measured result is found to be between the modelling results for a rear side Phong-scatterer with scattering angles of 18.0° and 25.2°. As mentioned in section 3 the model is purely empiric and does not really physically describe the structure and thus there will be a relevant error bar in the results. Due to this, in the following always the range between the two mentioned scattering angles will be given as a range instead of an exact result.

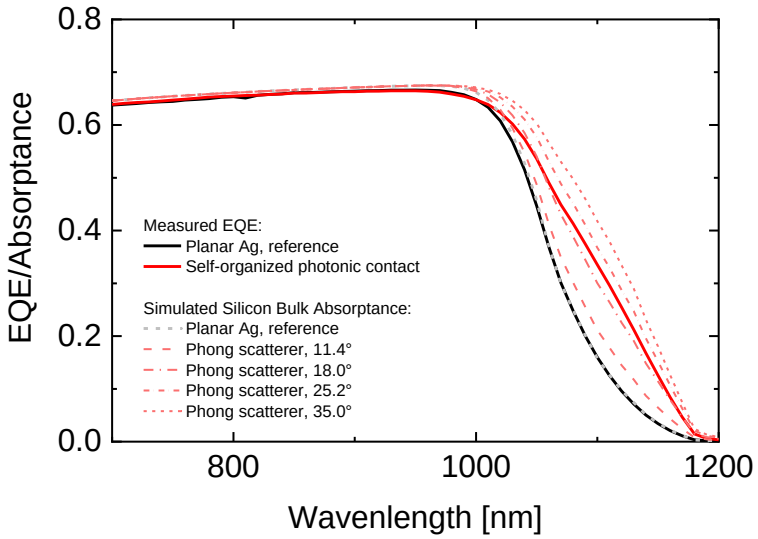

Figure 7 Comparison of EQE measurement and OPTOS modeling of the silicon bottom solar cell with self-organized photonic contact. The measured result is found to be in between the modelling results for rear side Phong-scatterers with scattering angles of 18.0° and 25.2°.

4.3 Estimation of current gain in thinner silicon cells

This model can in a second step be used to simulate the silicon bottom solar cell in a full tandem stack and estimate the potential current gain assuming different silicon bottom cell thicknesses. In detail two cell thicknesses were assumed: A 250 µm thick bottom solar cell, as similar cells are used to achieve the currently existing record devices, and a 150µm thick bottom solar cell, as this is in the range of the industrially realized silicon solar cells and thus more feasible for mass production. The results of these simulations are shown in Figure 8.
Calculating the bottom cell current density from the modeled absorptance assuming the AM1.5g spectrum and comparing this to the planar reference, the current gain for the 250µm thick solar cell is found to be between 1.1 mA/cm² and 1.4 mA/cm², which fits well to the measured current gain of 1.1 mA/cm².

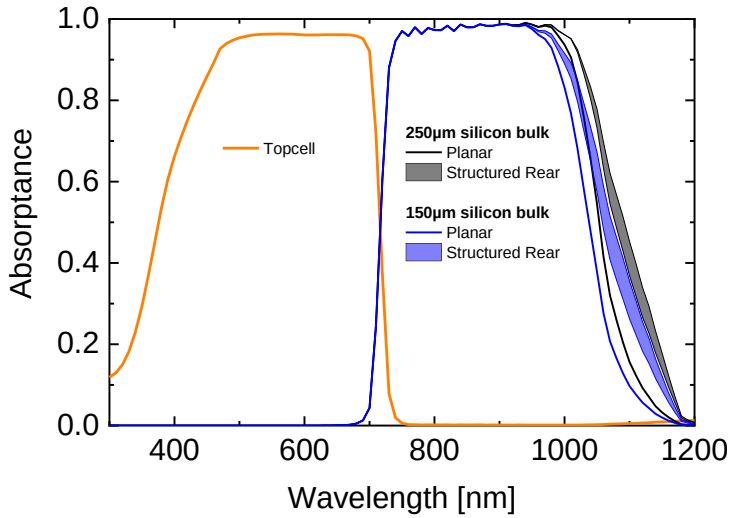

Figure 8 Absorptance in a silicon bottom solar cell with self-organized photonic contact, modeled as a Phong-scatterer for different cell thicknesses. Calculating the bottom cell current density from the modeled absorptance assuming the AM1.5g spectrum and comparing to the planar reference, the current gain for the 250µm thick solar cell is found to be between 1.1 mA/cm² and 1.4 mA/cm², which fits well to the measured current gain of 1.1 mA/cm². Assuming an industrially more relevant 150µm thick solar cell, one can expect a current gain in the range of 1.1-1.7 mA/cm².

Assuming an industrially more relevant 150µm thick solar cell, one can expect a current gain in the range of 1.1-1.7 mA/cm².
Note that random pyramids at the rear side can lead to an even higher current gain, while of course recombination will increase with the increased surface at random pyramids and thus the open circuit voltage will be influenced. Up to now it is not clear if the industrially realized random pyramids or a photonic contact will be the best option for the future. However, the self-organized photonic contact is an interesting alternative due to the extremely simple processing route in combination with the achieved remarkable current gain. Still, the currently necessary silver and the associated costs are one drawback. Reducing the amount of silver or replacing it has to be the next step.

5. CONCLUSION

It was shown that photonic contacts can improve the current of a silicon bottom solar cell significantly without deteriorating V_{oc} or FF. The self-organized photonic contact using phase-separation was found to allow for the same current gain as the much more complex NIL-based photonic contact using the same diffractive grating that was used in the current world record III-V on silicon tandem solar cells. Both concepts are promising candidates for the use as photonic contacts in different applications.

ACKNOWLEDGEMENT

The authors would like to express their gratitude to Volker Kübler, Sonja Seitz, Felix Schätzle, Frank Dimroth, Felix Predan, Christine Wellens, Adrian Callies at ISE for their support and input in many valuable discussions. This work has received funding from the European Union's Horizon 2020 research and innovation programme within the project SiTa-Sol under grant agreement No 727497 and by German Ministry for Economic Affairs and Energy through the project PoTaSi (no. 0324247). This article reflects only the authors' view and the funding agency is not responsible for any use that may be made of the information it contains.

REFERENCES

[1] F. Dimroth and K. Schneider, *Fraunhofer ISE Sets Two Records for the Efficiency of Silicon-Based Monolithic Triple-Junction Solar Cells*. Freiburg im Breisgau, 2019.

[2] R. Cariou, J. Benick, F. Feldmann, O. Höhn, H. Hauser, P. Beutel, N. Razek, M. Wimplinger, B. Bläsi, D. Lackner, M. Hermle, G. Siefer, S. W. Glunz, A. W. Bett, and F. Dimroth, "III–V-on-silicon solar cells reaching 33% photoconversion efficiency in two-terminal configuration," *Nature Energy*, vol. 3, no. 4, pp. 326–333, 2018.

[3] A. J. Wolf, H. Hauser, V. Kübler, C. Walk, O. Höhn, and B. Bläsi, "Origination of nano- and micro-structures on large areas by interference lithography," *Microelectron Eng*, vol. 98, no. 0, pp. 293–296, 2012.

[4] H. Hauser, B. Michl, S. Schwarzkopf, V. Kübler, C. Müller, M. Hermle, and B. Bläsi, "Honeycomb texturing of Silicon via nanoimprint lithography for solar cell applications," *IEEE Journal of Photovoltaics*, vol. 2, no. 2, pp. 114–122, 2012.

[5] N. Tucher, O. Höhn, H. Hauser, C. Müller, and B. Bläsi, "Characterizing the degradation of PDMS stamps in nanoimprint lithography," *Microelectronic Engineering*, vol. 180, pp. 40–44, 2017.

[6] A. Mellor, I. Tobias, A. Marti, M. J. Mendes, and A. Luque, "Upper limits to absorption enhancement in thick solar cells using diffraction gratings," (English), *Prog Photovoltaics*, vol. 19, no. 6, pp. 676–687, 2011.

[7] I. M. Peters, M. Rüdiger, H. Hauser, M. Hermle, and B. Bläsi, "Diffractive gratings for crystalline silicon solar cells-optimum parameters and loss mechanisms," *Prog. Photovolt: Res. Appl.*, vol. 20, no. 7, pp. 862–873, 2012.

[8] N. Tucher, J. Eisenlohr, P. Kiefel, O. Höhn, H. Hauser, I. M. Peters, C. Müller, J. C. Goldschmidt, and B. Bläsi, "3D optical simulation formalism OPTOS for textured silicon solar cells," *Opt. Express*, vol. 23, no. 24, pp. A1720, 2015.

[9] E. R. Martins, J. Li, Y. Liu, V. Depauw, Z. Chen, J. Zhou, and T. F. Krauss, "Deterministic quasi-random nanostructures for photon control," (eng), *Nat Comms*, vol. 4, p. 2665, 2013.

[10] M.-C. van Lare and A. Polman, "Optimized Scattering Power Spectral Density of Photovoltaic Light-Trapping Patterns," *ACS Photonics*, vol. 2, no. 7, pp. 822–831, 2015.

[11] C. Ton-That, A.G. Shard, and R.H. Bradley, “Surface feature size of spin cast PS/PMMA blends,” *Polymer*, vol. 43, no. 18, pp. 4973–4977, 2002.

[12] S. Walheim, M. Böltau, J. Mlynek, G. Krausch, and U. Steiner, “Structure Formation via Polymer Demixing in Spin-Cast Films,” *Macromolecules*, vol. 30, no. 17, pp. 4995–5003, 1997.

[13] Y. J. Donie, M. Smeets, A. Egel, F. Lentz, J. B. Preinfalk, A. Mertens, V. Smirnov, U. Lemmer, K. Bittkau, and G. Gomard, “Light trapping in thin film silicon solar cells via phase separated disordered nanopillars,” (eng), *Nanoscale*, vol. 10, no. 14, pp. 6651–6659, http://pubs.rsc.org/en/content/articlepdf/2018/NR/C8NR00455B, 2018.

[14] Hubert Hauser, Oliver Höhn, Ralph Müller, Nico Tucher, Kai Mühlbach, Rita Marlene da Silva Freitas, Jan Benick, Martin Hermle, and Benedikt Bläsi, “POLYMER-BASED REAR SIDE LIGHT TRAPPING STRUCTURES FOR SILICON-BASED TANDEM SOLAR CELLS,” in *Proceedings of the 36th European Photovoltaic Solar Energy Conference and Exhibition (EUPVSEC)*, Marseilles, France, 2019.

[15] J. Eisenlohr, B. G. Lee, J. Benick, F. Feldmann, M. Drießen, N. Milenkovic, B. Bläsi, J. C. Goldschmidt, and M. Hermle, “Rear side sphere gratings for improved light trapping in crystalline silicon single junction and silicon-based tandem solar cells,” *Solar Energy Materials & Solar Cells*, vol. 142, pp. 60–65, 2015.

[16] F. Feldmann, M. Bivour, C. Reichel, M. Hermle, and S. W. Glunz, “Passivated rear contacts for high-efficiency n-type Si solar cells providing high interface passivation quality and excellent transport characteristics,” *Solar Energy Materials & Solar Cells*, vol. 120, Part A, no. 0, pp. 270–274, 2014.

[17] M. Feifel, J. Ohlmann, J. Benick, M. Hermle, J. Belz, A. Beyer, K. Volz, T. Hannappel, A. W. Bett, D. Lackner, and F. Dimroth, “Direct Growth of III–V/Silicon Triple-Junction Solar Cells With 19.7% Efficiency,” *IEEE J. Photovoltaics*, vol. 8, no. 6, pp. 1590–1595, https://ieeexplore.ieee.org/ielx7/5503869/8511079/08467307.pdf?tp=&arnumber=8467307&isnumber=8511079, 2018.

[18] B. Bläsi, N. Tucher, O. Höhn, V. Kübler, T. Kroyer, C. Wellens, and H. Hauser, “Large area patterning using interference and nanoimprint lithography,” in *Proc. of SPIE*, Brussels, Belgium, 2016, p. 98880.

[19] B. Bläsi, H. Hauser, O. Höhn, V. Kübler, I. M. Peters, and A. J. Wolf, “Photon management structures originated by interference lithography,” in *Proceedings of the 1st International Conference on Crystalline Silicon Photovoltaics (SiliconPV)*, Freiburg; Germany, 2011, pp. 712–718.

[20] R. A. Sinton and A. Cuevas, “A quasi-steady-state open-circuit voltage method for solar cell characterization,” in *Proceedings of the 16th European Photovoltaic Solar Energy Conference (EUPVSEC)*, Glasgow, UK, 2000, pp. 1152–1155.

[21] T. Roth, J. Hohl-Ebinger, E. Schmich, W. Warta, S. W. Glunz, and R. A. Sinton, "Improving the accuracy of suns-VOC measurements using spectral mismatch correction," in *Proceedings of the 20st Workshop on Quantum Solar Energy Conversion*, Salzburg, Austria, 2008.

[22] O. Höhn, N. Tucher, A. Richter, M. Hermle, and B. Bläsi, "Light scattering at random pyramid textures: Effects beyond geometric optics," in *AIP Conf. Proc. 1999*, Lausanne, Switzerland, 2018, p. 30002.

[23] O. Höhn, N. Tucher, and B. Bläsi, "Theoretical study of pyramid sizes and scattering effects in silicon photovoltaic module stacks," (eng), *Opt. Express*, vol. 26, no. 6, A320, 2018.